





## Green biosynthesis, characterization, and cytotoxic effect of magnetic iron nanoparticles using *Brassica Oleracea var capitata sub var rubra* (red cabbage) aqueous peel extract

Ömer ERDOĞAN<sup>1</sup> , Salih PAŞA<sup>2</sup> , Gülen Melike DEMİRBOLAT<sup>3</sup> , Özge ÇEVİK<sup>1\*</sup>   
<sup>1</sup>Department of Biochemistry, Faculty of Medicine, Aydın Adnan Menderes University, Aydın, Turkey  
<sup>2</sup>Department of Science, Faculty of Education, Afyon Kocatepe University, Afyon, Turkey  
<sup>3</sup>Department of Pharmaceutical Technology, Faculty of Pharmacy, Biruni University, İstanbul, Turkey

Received: 01.02.2021 • Accepted/Published Online: 14.04.2021 • Final Version: 27.08.2021

**Abstract:** The green method of nanoparticle synthesis, which is an environment and living-friendly method, is an updated subject that has appeared as an alternative to conventional methods such as physical and chemical synthesis. In this presented study, the green synthesis of magnetic iron oxide nanoparticles (IONPs) from iron (III) chloride by using *Brassica oleracea var. capitata sub.var. rubra* aqueous peel extract has been reported. The prepared IONPs were characterized with fourier-transform infrared spectroscopy (FT-IR), ultraviolet-visible spectroscopy (UV-VIS), zeta potential, scanning electron microscopy (SEM), and energy-dispersive X-ray spectroscopy (EDX). The cytotoxic effects of IONPs on MCF-7 breast cancer cell line were studied by MTT assay, and migrative effect of its were carried out by the wound healing assay. It was found that the mean particle size of IONPs was  $675 \pm 25$  nm, and the polydispersity index was 0.265 PDI. It was also determined that these nanoparticles had an anti-proliferative impact on the MCF-7 breast cancer cell line depending on the dosage. Characterization results support the successful synthesis of nanoparticles, and the dose-dependent cytotoxic effects of nanoparticles on MCF-7 cells also make it a potential chemotherapeutic agent for breast cancer treatment.

**Keywords:** Green synthesis, iron oxide nanoparticles, red cabbage, *Brassica oleracea var. capitata sub.var. rubra*, breast cancer

### 1. Introduction

Nanotechnology is the one of up-to-date workspaces, which is aiming to develop materials with a range of 1–100 nm dimensions. With the development of nano-scale production, metal oxides like titanium dioxide (TiO<sub>2</sub>), silver oxide (AgO), gold oxide (AuO), copper oxide (CuO), iron oxide (FeO), zinc oxide (ZnO) have found wide application areas [1–3]. In biomedicine, iron oxide nanoparticles (IONPs) have various applications such as magnetic resonance imaging [4], isolation of proteins and DNA [5,6], drug delivery systems [7], cytotoxicity and anti-microbial studies [8–10]. Physical, chemical, and green synthesis methods are used extensively for the production of metal oxide nanoparticles. Physical methods require expensive material and equipment, high pressure and excessive temperature. In the chemical methods, toxic chemicals such as sodium borohydride and hydrazine hydrate are used as reducing agents, which can cause severe harm to the nature and to the alive [11–13]. On account of these disadvantages of chemical and physical methods, green synthesis is proposed to be an appropriate alternative to these methods. Bacteria, algae, fungi and plants are frequently preferred in the green synthesis of nanoparticles. Among these, plant extracts are more favorable because it decreases the hazard of more contamination by reducing the reaction time and preserving the cell structure. Medicinal plant extracts are a significant and generous source of bioactive compounds such as amino acids, proteins/enzymes, polysaccharides, fatty acids, and polyphenols that can perform cytotoxic activity in different cancer cell lines. On the other hand, these bioactive compounds can reduce positive charged metal ions and stabilize the nanoparticles to intended sizes and shapes [14,15].

To synthesize iron nanoparticles, the extract of *Lagenaria siceraria*, *Myrtus communis*, *Rhus punjabensis*, *Aesculus hippocatanum* were carried out in the recent past [16–19]. *Brassica oleracea var. capitata sub.var. rubra* is a autumn plant that grows almost anywhere in the world [20]. It has been reported that the red cabbage aqueous extract prepared by boiling method contains phenolic compounds, flavonoids, glucosinolates, sulforaphane, ascorbic acids, and anthocyanin pigments [21–23]. Also, it contains a high percentage of anthocyanin pigments that gives the specific color to red cabbage [24]. In the previous study conducted, it was determined that iron nanoparticles were synthesized using anthocyanin-

\* Correspondence: drozgecevik@gmail.com

rich-red cabbage extract and had an antimicrobial effect. It has been emphasized that the anthocyanins in the structure of red cabbage stabilize the structure of  $\text{Fe}_3\text{O}_4$  nanoparticles and increase their antimicrobial activity [10]. These metabolites are thought to facilitate the synthesis and stabilization of iron oxide nanoparticles. In the light of this information, iron oxide nanoparticles (IONPs) were synthesized using *Brassica oleracea var. capitata sub.var. rubra* peel extract, and their cytotoxic and wound closure effects were investigated on MCF-7 breast cancer cell lines.

## 2. Materials and method

### 2.1. The preparation of *Brassica oleracea var. capitata sub.var. rubra* peel extract

*Brassica oleracea var. capitata sub.var. rubra*, which weighs approximately 700 grams, harvested in the Aydin region were purchased from the marketplace in February 2020. Localization of market was  $37^{\circ}51'06.7''\text{N } 27^{\circ}48'33''\text{E}$ . *Brassica oleracea var. capitata sub.var. rubra* was peeled off. Then, gathered peels were washed 3 times with distilled water. Peels were chopped with a food processor. A total of 100 g of *Brassica oleracea var. capitata sub.var. rubra* peels and 200 mL distilled water were put into an erlenmeyer. This mixture was warmed up with a magnetic stirrer for 2 h at 100 °C. Finally, the mixture was filtered with Whatman filter paper (Grade1), and the filtrate was kept at +4 °C until it was used in nanoparticle synthesis. [25].

### 2.2. The synthesis of IONPs

20 mL of 10 mM iron (III) chloride solution and 10 mL of *Brassica oleracea var. capitata sub.var. rubra* peel extract was added in erlenmeyer. This mixture was ultrasonicated for 30 min. Then, it was exposed to 360 W microwave irradiation for 5 min. After the mixture was cooled to room temperature, the formed magnetic nanoparticles were attracted with a magnet, and the supernatant was discharged. The magnetic pellet was respectively washed five times with water and ethanol to eliminate organic residuals. After all, the pulverizing form of nanoparticles was gotten by drying in a 60 °C oven [26,27]. Illustration of IONPs synthesis with *Brassica oleracea var. capitata sub.var. rubra* peel extract was shown in Figure 1.

### 2.3. Characterization of IONPs

The ultraviolet-visible (UV-Vis) spectrum of iron nanoparticles was taken by spectrophotometer (Thermo Scientific Multiscan Spectrum 1500) with a range of 200–800 nm. The functional group analysis of IONPs was performed taking measurements in the range of 400–4000  $\text{cm}^{-1}$  with Fourier-transform infrared (FT-IR) spectrophotometer (Shimadzu IR 8000). Structural properties and surface morphological properties of IONPs were determined by scanning electron microscopy (SEM) (Zeiss LEO 1430 VP). Elemental composition analyses of IONPs were analyzed by energy-dispersive X-Ray (EDX) spectroscopy (LEO 1430 VP). Zeta potentials, particle distribution, and size of nanoparticles were determined using Zeta Sizer-Nano ZS (Malvern Instruments, England). Before the zeta measurement, nanoparticles were diluted with pure water and sonicated for 10 min.

### 2.4. Cell culture

MCF-7 breast cancer cells were grown and maintained in a 75  $\text{cm}^2$  flask with Dulbecco's Modified Eagle Medium (DMEM) medium including 10% FBS, 100  $\mu\text{g}/\text{mL}$  streptomycin, and 100  $\text{U}/\text{mL}^{-1}$  penicillin. The cultures were incubated with a humidified atmosphere, including 5%  $\text{CO}_2$ , at 37 °C. Culture medium was re-added with fresh medium every two days until catch up a proper confluency of about 90%. All medium and cell culture reagents were purchased from Gibco Company. Cell studies were repeated multiple times.

### 2.5. Antiproliferative assay

The effect of IONPs on breast cancer cell viability was determined using a based-on tetrazolium salt formation assay with MTT dyes. Shortly, the MCF-7 cells were seeded into a 96-well plate at a volume of  $1 \times 10^4$  cells/well. Cells were incubated for 24 h to adhere to the bottom of the wells. IONPs at different doses (1–1000  $\mu\text{g}/\text{mL}$ ) were added onto the cells and incubated during 24 h. Then, the culture medium in the wells was ejected, and the wells were washed with PBS three times. After fresh medium added to all wells, 10  $\mu\text{L}$  from MTT dye (0.5  $\text{mg}/\text{mL}$ ) were added to each well. The cells were kept in incubation for 4 h at 37°C. A total of 100  $\mu\text{L}$  DMSO was added per well to dissolve the formed formazan dye after discharging all the culture medium. The absorbance of each well was measured on a microplate reader (Biotek Co., USA) at the wavelength of 570 nm [28]. The % cell viability was calculated using the formula given below in equation (1).

$$\% \text{ Cell viability} = (\text{OD test sample}) / (\text{OD control}) \times 100 \quad (\text{Eq. 1})$$

### 2.6. Wound healing assay

Cells were seeded into a 12 well culture plate at a volume of  $1 \times 10^5$  cells/well. For the achieve confluence at the bottom of wells, cells were incubated overnight in DMEM medium. IONPs (100 and 1000  $\mu\text{g}/\text{mL}$ ) were added onto the cells and incubated for 24h. To modeling the wound formation, each well was drawn with the pipette tip in its mid-point. All wells were washed with PBS twice to suspend floating and non-adhering cells. Then, the fresh DMEM medium was added to

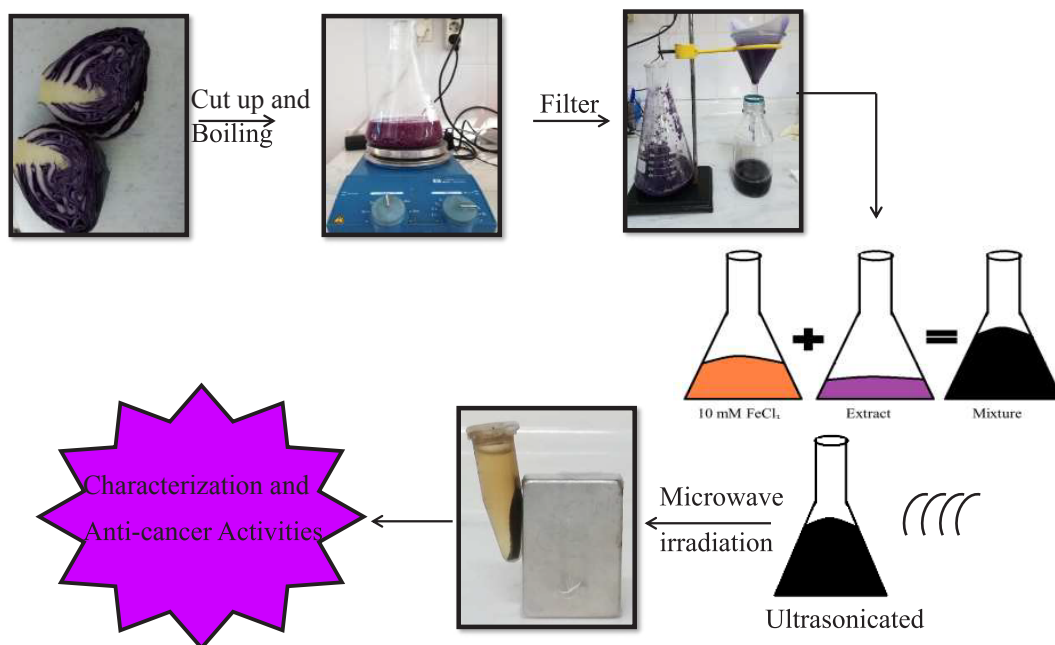


Figure 1. Illustration of IONPs synthesis.

each well. Subsequently, during 24 h, the cells migrated into the drawn zone were taken photography under an inverted microscope. The amount of 24-h wound closure relative to the onset time was calculated using the Image J program [29].

### 2.7. Apoptosis assay

The effect of IONPs on breast cancer cell apoptosis was determined with Annexin V & Dead Cell Kit using Muse cell analyzer. Cells were seeded into 6 well culture plates and treated with IONPs (100 and 1000  $\mu\text{g}/\text{mL}$ ) for 24h. After the incubation, the medium was emptied, and the cells were washed by PBS twice. Cells were removed using trypsin-EDTA and suspended with DMEM. Quickly, 100  $\mu\text{L}$  cell suspension and 100  $\mu\text{L}$  Annexin-V reagent were suspended and incubated for 20 min in the dark at room temperature. After, cells were measured for apoptosis and live cell count.

## 3. Results and discussion

### 3.1. Synthesized and characterization of synthesized IONPs

In recent years, plant extracts are more preferred in nanoparticle synthesis due to their inexpensive and environmentally friendly nature. When looking at the biosynthesis using red cabbage extract with different metal ions, copper [30], silver [31], and iron nanoparticles [10] stand out. Previous studies focused on the antioxidant and antimicrobial effects of these biosynthesis using aqueous red-cabbage extract. In this study, the anti-cancer effects of iron nanoparticles synthesized from red cabbage aqueous extract were investigated for the first time.

The altering color of the reaction environment (visual observation) throughout the reaction time is the prime sign of nanoparticle synthesis. This color altering emerges owing to the excitation of the surface plasmon on metal nanoparticles. To determine the effect of FeCl<sub>3</sub> concentration on nanoparticle synthesis, concentration of *Brassica oleracea var. capitata sub.var. rubra* extract was fixed for reaction. Nanoparticle synthesis was performed at 10 mM FeCl<sub>3</sub> since it gave the maximum reaction yield. After the leaf extract of *Brassica oleracea var. capitata sub.var. rubra* was added to the 10 mM ferric (II) sulfate solution, the color changed to dark black. The absorption spectrum 1  $\mu\text{g}/\text{mL}$ , 5  $\mu\text{g}/\text{mL}$ , 7.5  $\mu\text{g}/\text{mL}$  and 10  $\mu\text{g}/\text{mL}$  of IONPs spanned a wide range from 300 to 500 nm (Figure 2A). This band indicates the formation of IONPs because it is within the range of the surface plasmon resonance (SPR) for IONPs [32,33].

FTIR analysis is frequently preferred to identify the existence of functional groups on iron nanoparticles. The FTIR spectrum of IONPs show the prominent peaks at the 3358, 1608, 1419, 1330, 634, 576 and 457  $\text{cm}^{-1}$  wavenumbers (Figure 2B). The broad peak at 3385  $\text{cm}^{-1}$  is featured to hydrogen-bonded O-H stretching. The sharp peak at 1608  $\text{cm}^{-1}$  is assigned to C=O stretching vibrations. The sharp peaks of 1419 and 1330  $\text{cm}^{-1}$  are based on H-C-H vibration bending. Fe-O-Fe stretching vibrations were monitored at 634, 540 and 457  $\text{cm}^{-1}$  [34–36].

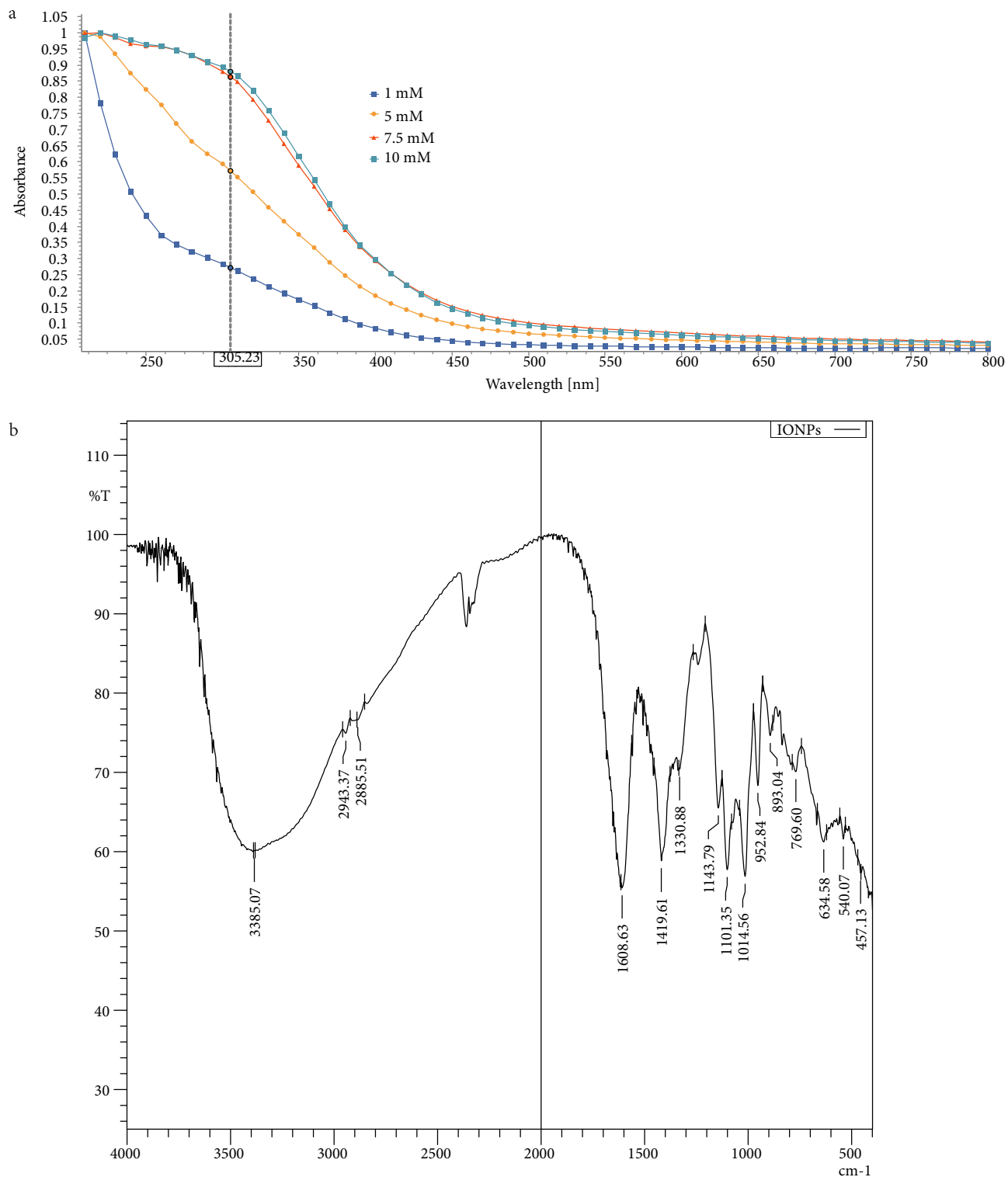


**Figure 2.** Characterization of synthesized IONPs. **A)** The UV-Vis spectrum of IONPs. **B)** The FTIR spectrum of IONPs.

Scanning electron microscopy technic has been utilized to determine the surface size and morphology of the IONPs [37–39]. Figure 3A shows the morphology of the iron nanoparticles synthesized by *Brassica oleracea var. capitata sub.var. rubra* aqueous extract. Agglomeration of IONPs may be caused owing to the swift loss of intermittent solvent [40]. Six hundred nm and 327 nm sized particles can be seen easily after 10000 times enlargement. The elemental scheme of IONPs

was calculated by using SEM accoutered with an energy dispersive X-Ray detector. EDX spectrum is shown the presence of iron nanoparticles as 12.94 % (Figure 3B). The other elements such as carbon, phosphorus, sulphur and sodium are probably caused by *Brassica oleracea var. capitata sub.var. rubra* residues on the iron nanoparticles [41,42]. Additionally, these elements exist naturally in the combination of red cabbage that also indicates the origin of growth [43].

Nanoparticles used for chemotherapy need to be absorbable to cell membranes. Some studies proposed that the size of nanoparticles exhibit a critical act in their fusion and passing to cell membranes. In general, particles with a particle size between 100–200 nm are usually taken into the cell by receptor-mediated endocytosis, whereas greater particles must be removed by phagocytosis [44,45]. In the case of evaluating the size of the iron nanoparticles synthesized by *Brassica oleracea var. capitata sub.var. rubra* leaf extract, it was obtained that the average particle size was  $675 \pm 25$  nm, and the polydispersity index was 0.265 PDI (Figure 4A). According to these results, IONPs are probably taken into phagocytosis into MCF-7 cells.

To understand how nanoparticles will behave in aqueous systems, the measurement of zeta potential or surface charge potential is a valuable data. The theoretical limit of stability of nanoparticles in a solvent system is  $\sim 30$  mV [46,47]. Zeta potential value of IONPs synthesized by *Brassica oleracea var. capitata sub.var. rubra* leaf extract determined as 9.59 mV (Figure 4B). This result clearly shows that IONPs synthesized by us are within the desired limits for stability.

### 3.2. Cell viability of MCF-7 cells treated with IONPs

Many studies have proved that plant extracts' bio components have cytotoxic activity against various cancerous and normal cell lines [48–50]. These bioactive components can pass to the surface of nanoparticles during the green synthesis process. Therefore, metal nanoparticles are frequently used in anticancer studies. Treatment of MCF-7 cells with 1–1000  $\mu\text{g}/\text{mL}$  doses of IONPs synthesized with *Brassica oleracea var. capitata sub.var. rubra* aqueous extract inhibited the proliferation of

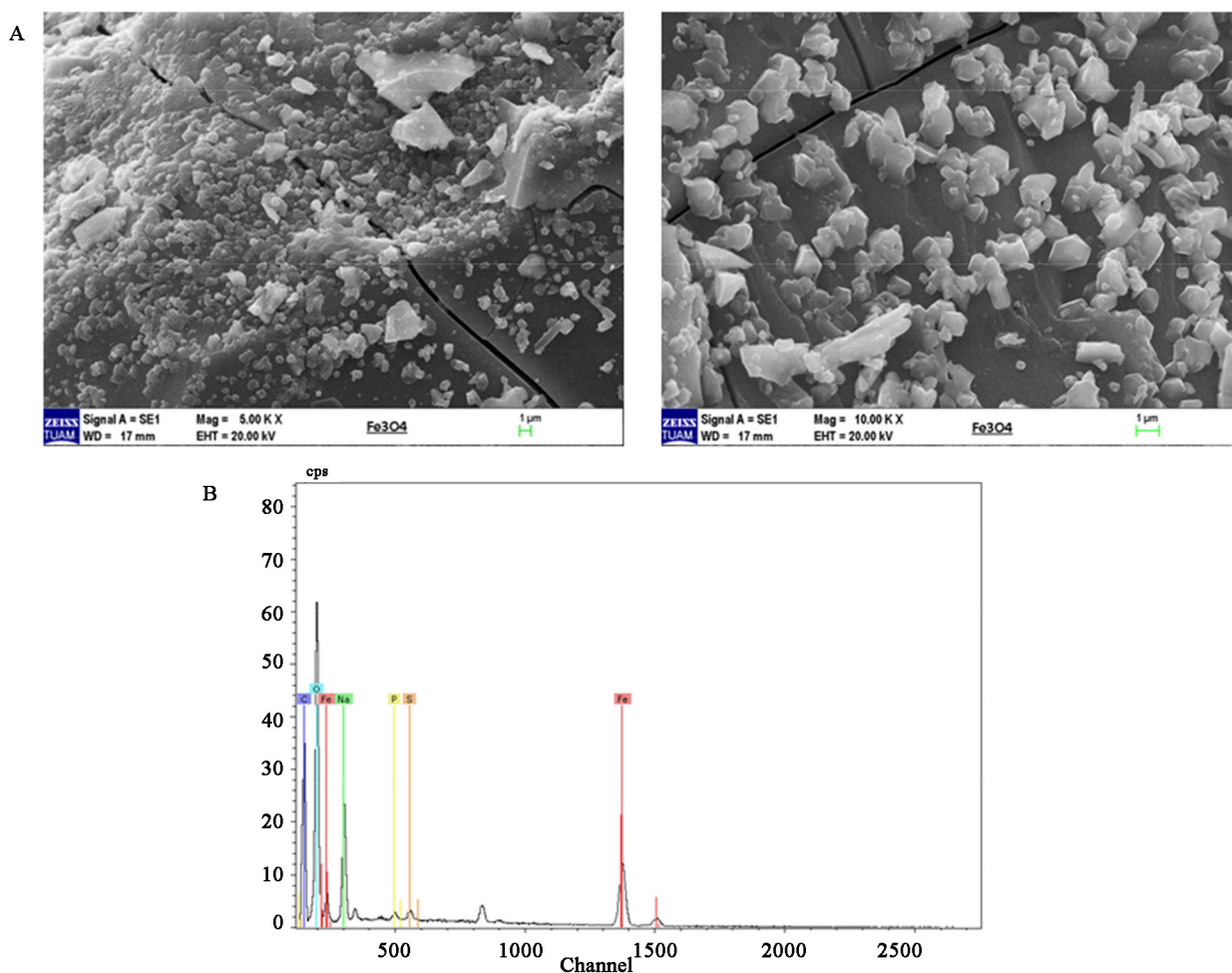
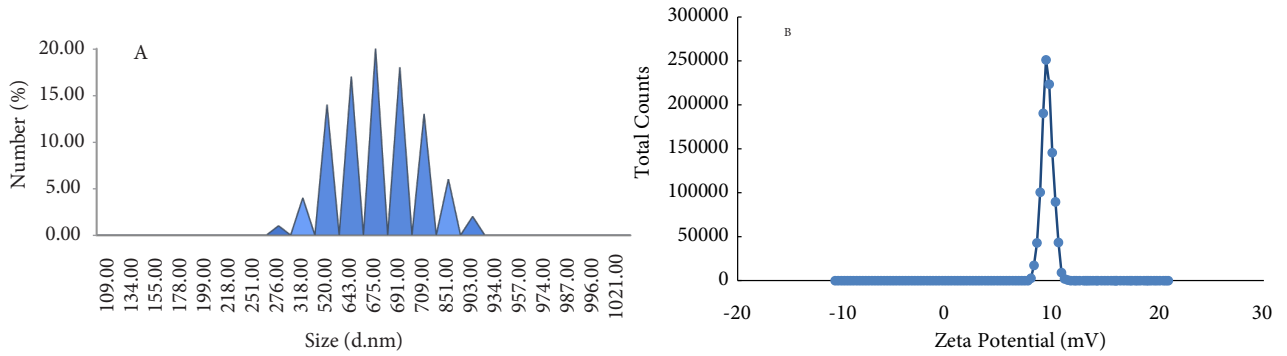
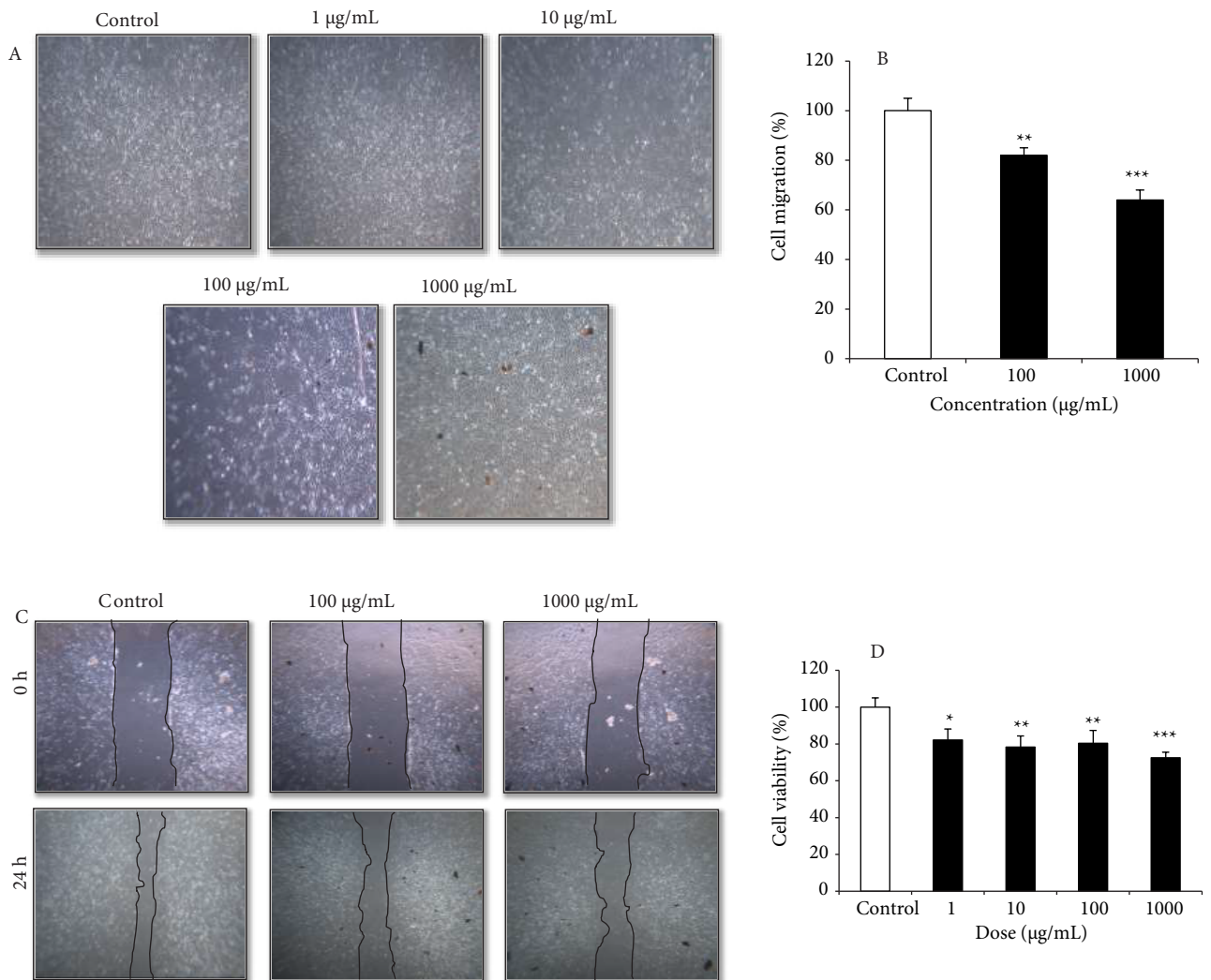


Figure 3. A) The SEM image of IONPs. B) Energy-dispersive X-ray spectroscopy (EDX) spectrum of IONPs



**Figure 4.** A) Size distribution and B) Zeta potential of IONPs.



**Figure 5.** The effect of IONPs in MCF-7 breast cancer cells. A) Cell morphological changes after treatment with 1–1000 µg/mL doses of IONPs in MCF-7 cell lines for 24 h. B) Graphical illustration of % cell survival rate of MCF-7 cells after treatment with 1–1000 µg/mL doses of IONPs. C) Scratch wound assay images of MCF-7 cells treated with 100–1000 µg/mL IONPs. D) The graphical illustration of wound closure area of MCF-7 cells after treatment with 100–1000 µg/mL IONPs (\*p < 0.05, \*\*p < 0.01, \*\*\*p < 0.001 compared to control cells).

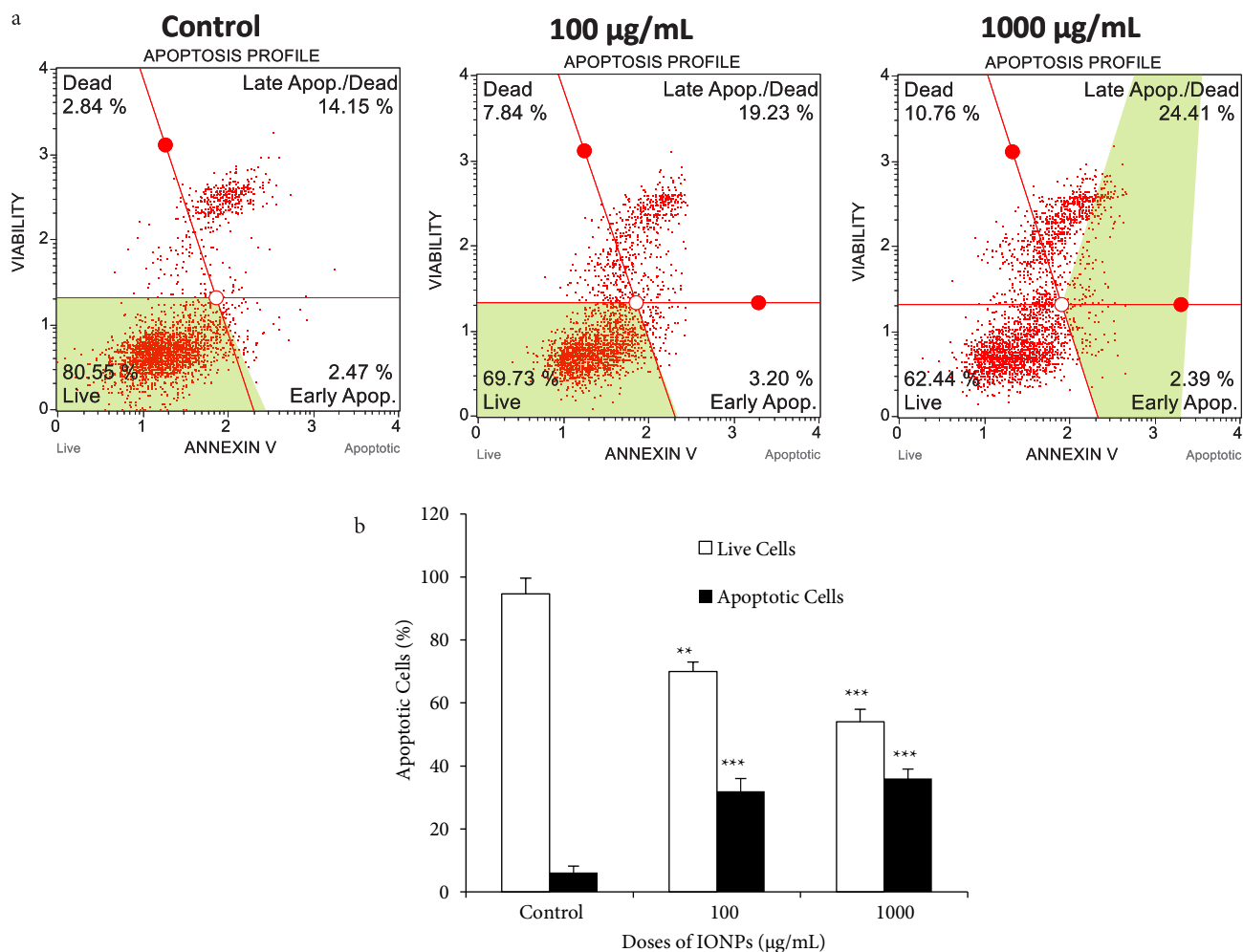


**Figure 6.** The apoptotic effect of IONPs in MCF-7 breast cancer cells. **A)** The scatter plot graphics of cells after treatment with 100 µg/mL and 1000 µg/mL doses of IONPs in MCF-7 cell lines for 24 h. **B)** The percentage of live and total apoptotic cells (early and late) of MCF-7 cells after treatment with 100 µg/mL and 1000 µg/mL doses of IONPs (\*\*p < 0.01, \*\*\*p < 0.001 compared to control cells).

the cells. When morphological images of the MCF-7 cells are examined (Figure 5A), it is observed that the cells treated with especially 100–1000 µg/mL IONPs show signs of apoptosis, such as blebbing the plasma membrane and shrinkage of the cell. Also, at these doses in the range of 100–1000 µg/mL, the cells move away from each other and float in the medium by rising from the well surface [51,52]. The results of MTT assay demonstrated that MCF-7 cells exposed to IONPs for 24 h resulted in concentration-dependent cytotoxicity. With increasing concentration of IONPs (1,10,100, 1000 µg/mL), the percentage viability was decreased from 100% to approximately 72.5% (Figure 5B). The results were supported by a study that iron nanoparticles synthesized with *Allium saracilum* extract could perform cytotoxic effect on HeLa and MCF-7 cells above 250 µg/mL and 500 µg/mL doses, respectively [53]. In another study, Zangeneh et al. stated that the 592 µg/mL dose of iron nanoparticles synthesized with *Falcaria vulgaris* extract reduced the cell viability of HUVEC cells to 50% [54]. Compared to this study, it appears that the iron nanoparticles synthesized with *Brassica oleracea var. capitata sub.var. rubra* leaf extract are more cytotoxic. Increased cytotoxic effect in our study is probably due to bioactive compounds from the *Brassica oleracea var. capitata sub.var. rubra* extract on the iron nanoparticle.

### 3.3. The effect of wound healing on MCF-7 cells treated with IONPS

Cancer cells have the ability to form colonies on their own and grow rapidly and form tumors in the tissue where they grow. Wound healing assay that measures of motility of cells is often used to determine the adhesion ability and metastatic potential of cancer cells. This method is constructed on observation of cell migration into a “wound” that is created on a cell monolayer [55]. Figure 5C shows the formed wounds at 0 h and the healing progression at 24 h in MKN-45 cells.

As shown in Figure 5D, cellular migration was inhibited by up to 87% and 27% at 24h with 100 µg/mL and 1000 µg/mL IONPs, respectively.

### 3.4. The effect of apoptosis on MCF-7 cells treated with IONPS

Measuring the percentage of cells leading to apoptosis is an important parameter in evaluating the cell health [56]. To investigate cells undergoing apoptosis, we carried out analysis with Annexin V assay. In cells undergoing apoptosis, the cell membrane asymmetry is lost, and phosphatidylserine is exposed on the membrane surface. In this case, phosphatidylserine and annexin-V binding are increased, so the number of apoptotic cells is detected [57]. After treated with 100 µg/mL and 1000 µg/mL IONPs, the percentage of total apoptotic MCF-7 cells respectively increased to 22.43% and 26.8% compared with control cells (Figure 6A). It was observed that the percentage of living cells decreased significantly in MCF-7 cells as a result of treatment with IONPs (Figure 6B,  $p < 0.001$ ). Marycz et al. reported similar results that 4B12 osteoclast cells treated with iron nanoparticles had a total apoptotic cell ratio of 29.75% [58]. It has been previously shown that hematite ( $\alpha\text{-Fe}_2\text{O}_3$ ) synthesized chemically without biosynthesis induces apoptosis in MCF-7 breast cancer cells in iron nanoparticles [59]. Many studies showed that metal nanoparticles enter the cell and induce oxidative stress, causing downregulation of anti-apoptotic proteins and triggering apoptosis in cancer cells by disrupting the plasma membrane structure [60].

## 4. Conclusion

IONPs are widely used in nanotechnology, biotechnology, and medical fields. In recent years, researchers have focused on the development of cost and time-effective methods for the synthesis of IONPs. In this study, which was performed with green synthesis, IONPs were synthesized using *Brassica oleracea var. capitata sub.var. rubra* leaf extract. In this way, both the physical methods that require expensive equipment are avoided and the chemical methods using chemicals that are harmful to the nature and living things. In addition, due to the cytotoxic effect of iron nanoparticles synthesized with *Brassica oleracea var. capitata sub.var. rubra* on MCF-7, cells may have the potential to be used as a chemotherapeutic agent in the cure of breast cancer.

## Acknowledgments

We thank ADU-BILTEM for providing laboratory and facility support for our research. This study was funded by Adnan Menderes University Research Grant (MARL-18001) given to Dr. Özge Çevik.

## References

1. Shabnam N, Pardha-Saradhi P. Photosynthetic electron transport system promotes synthesis of Au-nanoparticles. PLoS One 2013; 8 (8): e71123.
2. Erdoğan Ö, Birtokocak F, Oryaşın E, Abbak M, Demirebolat GM et al. Enginar yaprağı sulu ekstraktı kullanılarak çinko oksit nanopartiküllerinin yeşil sentezi, karakterizasyonu, anti-bakteriyel ve sitotoksik etkileri. Düzce Tıp Fakültesi Dergisi 2019; 21 (1): 19-26. (in Turkish).
3. Gunalan S, Sivaraj R, Venkatesh R. Aloe barbadensis Miller mediated green synthesis of mono-disperse copper oxide nanoparticles: optical properties. Spectrochimica Acta Part A: Molecular Biomolecular Spectroscopy 2012; 97: 1140-1144.
4. Pouliquen D, Le Jeune J, Perdrisot R, Ermias A, Jallet P. Iron oxide nanoparticles for use as an MRI contrast agent: pharmacokinetics and metabolism. Magnetic Resonance Imaging 1991; 9 (3): 275-283.
5. Okoli C, Fornara A, Qin J, Toprak MS, Dalhammar G et al. Characterization of superparamagnetic iron oxide nanoparticles and its application in protein purification. Journal of Nanoscience Nanotechnology 2011; 11 (11): 10201-10206.
6. Saiyed Z, Ramchand C, Telang S. Isolation of genomic DNA using magnetic nanoparticles as a solid-phase support. Journal of Physics: Condensed Matter 2008; 20 (20): 204153.
7. Vangijzegem T, Stanicki D, Laurent S. Magnetic iron oxide nanoparticles for drug delivery: applications and characteristics. Expert Opinion on Drug Delivery 2019; 16 (1): 69-78.
8. Mahmoudi M, Simchi A, Imani M, Shokrgozar MA, Milani AS et al. A new approach for the in vitro identification of the cytotoxicity of superparamagnetic iron oxide nanoparticles. Colloids Surfaces B: Biointerfaces 2010; 75 (1): 300-309.
9. Saranya S, Vijayarani K, Pavithra S. Green synthesis of iron nanoparticles using aqueous extract of Musa ornata flower sheath against pathogenic bacteria. Indian Journal of Pharmaceutical Sciences 2017; 79 (5): 688-694.
10. Demirbas A, Kislakci E, Karaagac Z, Onal I, Ildiz N et al. Preparation of biocompatible and stable iron oxide nanoparticles using anthocyanin integrated hydrothermal method and their antimicrobial and antioxidant properties. Materials Research Express 2019; 6 (12): 125011.



11. Khan ST, Musarrat J, Al-Khedhairi AA. Countering drug resistance, infectious diseases, and sepsis using metal and metal oxides nanoparticles: current status. *Colloids Surfaces B: Biointerfaces* 2016; 146: 70-83.
12. Agarwal H, Kumar SV, Rajeshkumar S. A review on green synthesis of zinc oxide nanoparticles–An eco-friendly approach. *Resource-Efficient Technologies*. 2017; 3 (4): 406-413.
13. Saif S, Tahir A, Chen Y. Green synthesis of iron nanoparticles and their environmental applications and implications. *Nanomaterials* 2016; 6 (11): 209.
14. Devatha C, Thalla AK, Katte SY. Green synthesis of iron nanoparticles using different leaf extracts for treatment of domestic waste water. *Journal of Cleaner Production* 2016; 139: 1425-1435.
15. Farshchi HK, Azizi M, Jaafari MR, Nemati SH, Fotovat A. Green synthesis of iron nanoparticles by Rosemary extract and cytotoxicity effect evaluation on cancer cell lines. *Biocatalysis Agricultural Biotechnology* 2018; 16: 54-62.
16. Kanagasubbulakshmi S, Kadirvelu K. Green synthesis of iron oxide nanoparticles using *Lagenaria siceraria* and evaluation of its antimicrobial activity. *Defence Life Science Journal* 2017; 2 (4): 422-427.
17. Eslami S, Ebrahimzadeh MA, Biparva P. Green synthesis of safe zero valent iron nanoparticles by *Myrtus communis* leaf extract as an effective agent for reducing excessive iron in iron-overloaded mice, a thalassemia model. *RSC Advances* 2018; 8 (46): 26144-26155.
18. Naz S, Islam M, Tabassum S, Fernandes NF, de Blanco EJC et al. Green synthesis of hematite ( $\alpha$ -Fe<sub>2</sub>O<sub>3</sub>) nanoparticles using *Rhus punjabensis* extract and their biomedical prospect in pathogenic diseases and cancer. *Journal of Molecular Structure* 2019; 1185: 1-7.
19. Demirezen DA, Yilmaz D, Yilmaz Ş. Green synthesis and characterization of iron nanoparticles using *Aesculus hippocastanum* seed extract. *Int J Adv Sci Eng Technol* 2018; 6: 2321-8991.
20. Kent NK, Cengiz S. The impacts of kale extracts on the levels of malondialdehyde in invitro oxide lipoproteins. *Gümüşhane University Journal of Health Sciences* 2016; 5 (2): 42-47.
21. Tabart J, Pincemail J, Kevers C, Defraigne JO, Dommes J. Processing effects on antioxidant, glucosinolate, and sulforaphane contents in broccoli and red cabbage. *European Food Research Technology* 2018; 244 (12): 2085-2094.
22. Bilyk A, Sapers GM. Distribution of quercetin and kaempferol in lettuce, kale, chive, garlic chive, leek, horseradish, red radish, and red cabbage tissues. *Journal of Agricultural Food Chemistry* 1985; 33 (2): 226-228.
23. Phahlane CJ, Maboko MM, Soundy P, Sivakumar D. Development, yield, and antioxidant content in red cabbage as affected by plant density and nitrogen rate. *International Journal of Vegetable Science* 2018; 24 (2): 160-168.
24. Ahmadiani N, Robbins RJ, Collins TM, Giusti MM. Anthocyanins contents, profiles, and color characteristics of red cabbage extracts from different cultivars and maturity stages. *Journal of Agricultural Food Chemistry* 2014; 62 (30): 7524-7531.
25. Rao KG AC, Rao KV, Chakra CHS, Akshaykranth A. . Eco-friendly synthesis of MgO nanoparticles from orange fruit waste. *International Journal of Advanced Research in Physical Science* 2015; 2 (3): 1-6.
26. Joseph S, Mathew B. Microwave-assisted green synthesis of silver nanoparticles and the study on catalytic activity in the degradation of dyes. *Journal of Molecular Liquids* 2015; 204: 184-191.
27. Haris M, Kumar A, Ahmad A, Abuzinadah MF, Basheikh M et al. Microwave-assisted green synthesis and antimicrobial activity of silver nanoparticles derived from a supercritical carbon dioxide extract of the fresh aerial parts of *Phyllanthus niruri* L. *Tropical Journal of Pharmaceutical Research* 2017; 16 (12): 2967-2976.
28. Cevik O, Turut FA, Acidereli H, Yildirim S. Cyclosporine-A induces apoptosis in human prostate cancer cells PC3 and DU145 via downregulation of COX-2 and upregulation of TGF $\beta$ . *Turkish Journal of Biochemistry* 2018; 44 (1): 47-54.
29. Erdogan O, Abbak M, Demirbolat GM, Birtekocak F, Aksel M et al. Green synthesis of silver nanoparticles via *Cynara scolymus* leaf extracts: The characterization, anticancer potential with photodynamic therapy in MCF7 cells. *PLoS One* 2019; 14 (6): e0216496.
30. Fernandez AC, Archana K. Green synthesis, characterization, catalytic and antibacterial studies of copper iodide nanoparticles synthesized using *Brassica oleracea* var. *capitata* f. *rubra* extract. *Chemical Data Collections* 2020; 29: 100538.
31. Ocsoy I, Demirbas A, McLamore ES, Altinsoy B, Ildiz N et al. Green synthesis with incorporated hydrothermal approaches for silver nanoparticles formation and enhanced antimicrobial activity against bacterial and fungal pathogens. *Journal of Molecular Liquids* 2017; 238: 263-269.
32. Luo F, Chen Z, Megharaj M, Naidu R. Biomolecules in grape leaf extract involved in one-step synthesis of iron-based nanoparticles. *RSC Advances* 2014; 4 (96): 53467-53474.
33. Mohanraj S, Kodhaiyolii S, Rengasamy M, Pugalenti V. Green synthesized iron oxide nanoparticles effect on fermentative hydrogen production by *Clostridium acetobutylicum*. *Applied biochemistry biotechnology* 2014; 173 (1): 318-331.

34. Thenmozhi B SS, Sudha R, Revathy B. Green synthesis and comparative study of silver and iron nanoparticle from leaf extract. *Int J Inst Pharm Life Sci* 2014; 4: 5-12.
35. Wang T, Lin J, Chen Z, Megharaj M, Naidu R. Green synthesized iron nanoparticles by green tea and eucalyptus leaves extracts used for removal of nitrate in aqueous solution. *Journal of cleaner production* 2014; 83: 413-419.
36. Huang L, Weng X, Chen Z, Megharaj M, Naidu R. Synthesis of iron-based nanoparticles using oolong tea extract for the degradation of malachite green. *Spectrochimica Acta Part A: Molecular Biomolecular Spectroscopy* 2014; 117: 801-804.
37. Jebali A, Ramezani F, Kazemi B. Biosynthesis of silver nanoparticles by *Geotricum* sp. *Journal of Cluster Science* 2011; 22 (2): 225-232.
38. Devi HS, Boda MA, Shah MA, Parveen S, Wani AH. Green synthesis of iron oxide nanoparticles using *Platanus orientalis* leaf extract for antifungal activity. *Green Processing Synthesis* 2019; 8 (1): 38-45.
39. Beheshtkhou N, Kouhbanani MAJ, Savardashtaki A, Amani AM, Taghizadeh S. Green synthesis of iron oxide nanoparticles by aqueous leaf extract of *Daphne mezereum* as a novel dye removing material. *J Applied Physics A* 2018; 124 (5): 1-7.
40. Handore K, Bhavsar S, Horne A, Chhattise P, Mohite K et al. Novel green route of synthesis of ZnO nanoparticles by using natural biodegradable polymer and its application as a catalyst for oxidation of aldehydes. *Journal of Macromolecular Science, Part A* 2014; 51 (12): 941-947.
41. Ma M, Zhang Y, Yu W, Shen H, Zhang H, et al. Preparation and characterization of magnetite nanoparticles coated by amino silane. *Colloids Surfaces A: physicochemical engineering aspects* 2003; 212 (2-3): 219-226.
42. Shahwan T, Sirriah SA, Nairat M, Boyacı E, Eroğlu AE et al. Green synthesis of iron nanoparticles and their application as a Fenton-like catalyst for the degradation of aqueous cationic and anionic dyes. *Chemical Engineering Journal* 2011; 172 (1): 258-266.
43. Bong YS, Shin WJ, Gautam MK, Jeong YJ, Lee AR et al. Determining the geographical origin of Chinese cabbages using multielement composition and strontium isotope ratio analyses. *Food chemistry* 2012; 135 (4): 2666-2674.
44. Couvreur P, Puisieux F. Nano- and microparticles for the delivery of polypeptides and proteins. *Advanced Drug Delivery Reviews* 1993; 10 (2-3): 141-162.
45. Win KY, Feng SS. Effects of particle size and surface coating on cellular uptake of polymeric nanoparticles for oral delivery of anticancer drugs. *Biomaterials* 2005; 26 (15): 2713-2722.
46. Ebrahiminezhad A, Zare-Hoseinabadi A, Berenjian A, Ghasemi Y. Green synthesis and characterization of zero-valent iron nanoparticles using stinging nettle (*Urtica dioica*) leaf extract. *Green Processing Synthesis* 2017; 6 (5): 469-475.
47. Duman O, Tunç S. Electrokinetic and rheological properties of Na-bentonite in some electrolyte solutions. *Microporous Mesoporous Materials* 2009; 117 (1-2): 331-338.
48. Saranya S, Vijayarani K, Pavithra S, Raihana N, Kumanan K. In vitro cytotoxicity of zinc oxide, iron oxide and copper nanopowders prepared by green synthesis. *Toxicology Reports* 2017; 4: 427-430.
49. Lourenço IM, Pieretti JC, Nascimento MHM, Lombello CB, Seabra AB. Eco-friendly synthesis of iron nanoparticles by green tea extract and cytotoxicity effects on tumoral and non-tumoral cell lines. *Energy, Ecology and Environment* 2019; 4 (6): 261-270.
50. Chavan RR, Bhinge SD, Bhutkar MA, Randive DS, Wadkar GH et al. Characterization, antioxidant, antimicrobial and cytotoxic activities of green synthesized silver and iron nanoparticles using alcoholic *Blumea eriantha* DC plant extract. *Materials Today Communications* 2020; 24: 101320.
51. Kettmann V, Košťálová D, Jantova S, Čerňáková M. In vitro cytotoxicity of berberine against HeLa and L1210 cancer cell lines. *Die Pharmazie- An International Journal of Pharmaceutical Sciences* 2004; 59 (7): 548-551.
52. Senff-Ribeiro A, Echevarria A, Silva E, Franco C, Veiga S et al. Cytotoxic effect of a new 1,3,4-thiadiazolium mesoionic compound (MI-D) on cell lines of human melanoma. *British journal of cancer* 2004; 91 (2): 297-304.
53. Zangeneh A, Zangeneh MM, Moradi R. Ethnomedicinal plant-extract-assisted green synthesis of iron nanoparticles using *Allium saralicum* extract, and their antioxidant, cytotoxicity, antibacterial, antifungal and cutaneous wound-healing activities. *Applied Organometallic Chemistry* 2019; 34: e5254.
54. Zangeneh MM, Zangeneh A, Pirabbasi E, Moradi R, Almasi M. *Falcaria vulgaris* leaf aqueous extract mediated synthesis of iron nanoparticles and their therapeutic potentials under in vitro and in vivo condition. *Applied Organometallic Chemistry* 2019; 33 (12): e5246.
55. Rodriguez LG, Wu X, Guan JL. Wound-healing assay. *Cell Migration*. Springer; 2005. p. 23-29.
56. Khan A, Gillis K, Clor J, Tyagarajan K. Simplified evaluation of apoptosis using the Muse cell analyzer. *Postepy biochemii* 2012; 58 (4): 492-496.
57. Logue SE, Elgendy M, Martin SJ. Expression, purification and use of recombinant annexin V for the detection of apoptotic cells. *Nature protocols* 2009; 4 (9): 1383.

58. Marycz K, Sobierajska P, Roecken M, Kornicka-Garbowska K, Kępska M et al. Iron oxides nanoparticles (IOs) exposed to magnetic field promote expression of osteogenic markers in osteoblasts through integrin alpha-3 (INTa-3) activation, inhibits osteoclasts activity and exerts anti-inflammatory action. *Journal of nanobiotechnology* 2020; 18 (1): 1-24.
59. Kanagesan S, Hashim M, Tamilselvan S, Alitheen N, Ismail I et al. Synthesis, characterization, and cytotoxicity of iron oxide nanoparticles. *Advances in Materials Science Engineering* 2013; 2013: 710432.
60. Jacob JA, Salmani JMM, Chen B. Magnetic nanoparticles: mechanistic studies on the cancer cell interaction. *Nanotechnology Reviews* 2016; 5 (5): 481-488.